Mathematical Model for Osteobstruction in Bone Regeneration Mechanisms A Headway in Skeletal Tissue Engineering

C Ogunsalu[1], FI Arunaye[2], C Ezeokoli[3], M Gardner[1], M Rohrer[4], H Prasad[4]

ABSTRACT

In this paper, we formulate a mathematical model for the evaluation of parameters responsible for the retardation and eventual acceleration of bone regeneration on the contralateral side of the mandible of experimental animals, following the discovery of a new mechanism of bone regeneration called the osteobstruction mechanism (a negative mechanism of bone regeneration as opposed to the well established and extensively documented positive mechanisms such as osteogenesis, osteoinduction and osteoconduction). This osteobstructive mechanism was demonstrated by episodes of overtaking and re-overtaking on single photon emission computed tomography (SPECT) following evaluation of osteoblastic activities in a sequential animal experiment to validate both the Ogunsalu sandwich technique (a double guided tissue technique; D-GTR) and the interceed membrane technique (a single guided tissue regeneration technique; S-GTR) utilizing SPECT, histological and histomorphometric evaluation. This work is now given special attention in terms of mathematical analysis because of limited experimental observations since experiments cannot be observed infinitely. Mathematical modelling is as such essential to generalize the results of this osteobstructive mechanism in bone regeneration. We utilize the Fisher's equation to describe bone cell mobilization during bone regeneration by two different techniques: the Ogunsalu sandwich bone regeneration technique (D-GTR) and the S-GTR.

Keywords: Bone regeneration, mathematical model, osteobstruction

Modelo Matemático de la Osteobstrucción en el Mecanismo de Regeneración del Hueso: Un Avance en la Ingeniería del Tejido Esquelético

C Ogunsalu[1], FI Arunaye[2], C Ezeokoli[3], M Gardner[1], M Rohrer[4], H Prasad[4]

RESUMEN

En este trabajo se formula un modelo matemático para la evaluación de los parámetros responsables del retardo y la posterior aceleración de la regeneración del hueso en el lado contralateral de la mandíbula de animales experimentales, tras el descubrimiento de un nuevo mecanismo de regeneración del hueso, denominado mecanismo de osteobstrucción de la regeneración del hueso (un mecanismo negativo de regeneración del hueso, el cual contrasta con mecanismos positivos bien establecidos y ampliamente documentados, tales como la osteogénesis, la osteoinducción y la osteoconducción). Este mecanismo osteobstructivo fue demostrado mediante una serie de fenómenos consecutivos en la tomografía computarizada por Emisión de Fotones Individuales (SPECT), tras la evaluación actividades osteoblásticas en experimentos secuenciales con animales, para validar tanto la técnica de

From: [1]Section of Anatomy, Department of Basic Medical Sciences, Faculty of Medical Sciences, [2]Department of Mathematics and Computer Science, Faculty of Science and Technology, The University of the West Indies, Kingston 7, Jamaica, [3]School of Veterinary Medicine, Faculty of Medical Sciences, The University of the West Indies, St Augustine, Trinidad and Tobago and [4]Department of Pathology, University of Minnesota, Minnesota, United States of America.

Correspondence: Dr C Ogunsalu, Section of Anatomy, Department of Basic Medical Sciences, Faculty of Medical Sciences, The University of the West Indies, Kingston 7, Jamaica. E-mail: chrisogun@yahoo.com

Footnote: The abstract of this paper was previously published in Oral Surg Oral Med Oral Pathol Oral Radiol Endod 2010; **110:** 315–16. It may be viewed at http://dx.doi.org/10.1016/j.tripleo.2010.05.024

sandwich de Ogunsalu (técnica de regeneración de tejidos guiada doble; RTG-D) como la técnica de membrana con interceed (técnica de regeneración de tejidos guiada simple; RTG-S) utilizando SPECT así como evaluaciones histológicas e histomorfométricas. Este trabajo recibe aquí especial atención en términos de análisis matemático, ya que en los experimentos las observaciones no puede realizarse infinitamente. Los modelos matemáticos son pues esenciales para generalizar los resultados de este mecanismo del osteobstructivo de la regeneración ósea. Se utiliza la ecuación de Fisher para describir la movilización de las células óseas durante la regeneración del hueso por dos técnicas diferentes: la técnica de Ogunsalu para la regeneración ósea por "sandwich" (D-GTR) y la técnica S-GTR.

Palabras claves: Regeneración del hueso, modelo matemático, osteobstrucción

West Indian Med J 2012; 61 (8): 815

INTRODUCTION

The osteobstruction mechanism in bone regeneration was coincidentally discovered during a sequential single photon emission computed tomography (SPECT), histological and histomorphometric analysis on animal model in the validation of the Ogunsalu sandwich bone regeneration technique (1–3). Mathematical models are essential for refining laboratory/clinical experimental data since such experimental observations are subject to time constraint. Bone regeneration, an important phenomenon in mathematical biology/tissue engineering, has attracted desirable attention in the literature (4–11). The common assumption in the literature is that bone or tissue can only be generated if the concentration of the growth factor exceeds a certain threshold value (7, 12). The expressions for the equation of motion and the distribution of the growth factor are usually related in a way that no bone formation (healing) occurs if the growth factor concentration is below a certain value (12). Mathematical models in the bone regeneration mechanism which incorporate cell mitosis, cell proliferation, cell death, capillary density, oxygen supply and growth factor regeneration coupled to a cell density, have all been recently studied and documented (13–16).

Generally, cell ingrowth may be retarded by various constraints *ie* pore size of porous biomaterials for bone graft, unfavourable surface characteristics, or may be counteracted by chemotactic movement towards external supplies of nutrients and other important biochemical factors (7). Tissue ingrowth can also be enhanced by applying surface modifications to the biomaterial (17–20). Systematic approach to cell motility can be studied in two-dimensional or three-dimensional cell adhesion (7, 21). Mathematical modelling is essential in biological systems/tissue engineering to predict, interpret and generalize the results of clinical experiments and also to derive the intrinsic parameters that can be used to predict cell behaviour (4, 22).

It is well known that in the formulation of mathematical model, based upon the interactions of individual cells, it is required that the position and velocity of each individual cell within the system be considered. Individual cell-based models comparatively provide comprehensive and detailed information about the dynamics of the cell population and as well offer distinct advantages over continuum-based models (7, 23). However, these models are relatively complex due to the fact that rules governing cell behaviour and the ability to track the movement of individual cells is extremely tedious and difficult (7, 23). It is also well known that the continuum-based model (23) allows mathematical expressions that exploit partial differential equations (PDEs), and hence are amenable to PDE theory for analytic or asymptotic solutions as well as numerical simulations.

General conceptualization of transport model in fluid mechanic, physical or biological mathematical modelling assumed the usual diffusion model $\frac{\partial X}{\partial t} - d\nabla^2 X + q$ [1] where X represents concentration, d is the diffusion coefficient and q is the death and birth (consumption and synthesis) rate of the biological phenomenon that is on motion (migration); usually governed by $q = \gamma(1 - \frac{X}{X_\circ})X$ [2] and $X_\circ$ is the maximum concentration, γ is the proliferation rate. The predicted concentration X is known to be in good qualitative agreement with laboratory experiment (4, 24).

The well known Fisher's equation $\frac{\partial B}{\partial t} - \nabla \cdot (D\nabla B) + R(1 - \frac{B}{B_\infty})B$ [3] has been used to represent experimental data from bone regeneration (wound-healing, gene transportation *etc* as the case may be) experiment (4, 5, 7). This mathematical model [3] has very wide applications particularly in the area of cell transportation in bioengineering and has proved formidable (4, 5, 7). Equation 3 describes the behaviour of a cell population (continuum-based model) as a combination of random cell motion and logistic proliferation (proliferation up to a maximum cell density). The condition on cell motility takes the form of a travelling wave of fixed shape that propagates at constant speed (23–25). The velocity depends only on a simple combination of the motility coefficient and the proliferation rate. Thus with

given motility front velocity determined experimentally, it is easy to derive the motility coefficient if the proliferation rate is known (7, 24). Recently, a series of mathematical models suitable for describing biological tissue growth *in vitro* was developed (23); these models investigated the influence of cell-cell and cell-scaffold interactions and the mechanical environment on tissue growth *in vitro* tissue engineering (23). In this paper, we formulate mathematical models for the Ogunsalu osteobstruction phenomenon.

MATERIAL AND METHOD

After the observation of the osteobstructive phenomenon/mechanism and its cumulative SPECT, histological and histomorphometric evaluation (1–3), the Fisher's equation [3] was utilized to speculate the bone cell concentration variable and other parameters. We also assumed that the sandwich membrane bag of the Ogunsalu double guided tissue technique (D-GTR) is cubic of unit sides and the dimension of the single guided tissue technique (S-GTR) is unit side square membrane.

Mathematical models for osteobstruction

Single GTR model

The area of membrane of square width L is $L \times L = L^2$ unit square, osteobstruction parameter is λ_1 unit square per second, per second is the measure of soft tissue layer at graft site, effect of membrane/tissue interaction is ξ (real variable).

The presence of λ_1 activates negative flow of cells to graft site *ie* negative sign of diffusivity coefficient, thus we have $D_1 = -D$ where D_1 is the coefficient of diffusivity when λ_1 is present; D is the coefficient of diffusivity of the standard Fisher's equation.

We modelled the relation between the rate of bone cell proliferation R_1 at graft site when λ_1 is present and that of the standard Fisher's equation (23) rate of bone cell proliferation R at graft site in the absence of osteobstructivity as

$$R_1 - \left(\frac{1+\xi\lambda_1}{1-\lambda_1}\right)R \quad [4].$$

The retardation effect on bone cell proliferation is obtained by ensuring that $\frac{1+\xi\lambda_1}{1-\lambda_1} > 0 \Rightarrow \xi < \frac{1}{\lambda_1}$ [5]. We define the general osteobstruction parameter in the two states of GTR by the relation λ_m = *surface area of membrane for GTR – 3m; m* = 1,2 [6]

ie: $\lambda_1 - L^2 \quad 3 - \quad 2; L - 1 \rightarrow \xi < \frac{1}{2}$ [7].

Double GTR (Ogunsalu sandwich GTR) model

In this case, we have $\lambda_2 = 6L^2 - 6 = 0$; $L = 1$ *ie* the value of osteobstruction parameter is zero when $m = 2$ in equation 6. So $D_2 = D$ and $R_2 = R$. We observed from the SPECT that the effect of resorption of D-GTR membrane and some biochemical reaction produced a sudden drop in bone cell concentration which we denoted by $\in \lambda_\circ$ (real number).

RESULTS

The sequential SPECT is shown in Figs 1–6 with evidence of osteobstruction between the 11th week (Fig. 2) and the 13th week (Fig. 3). The osteobstruction was positively correlated with the occurrence of foreign body reaction on histology at

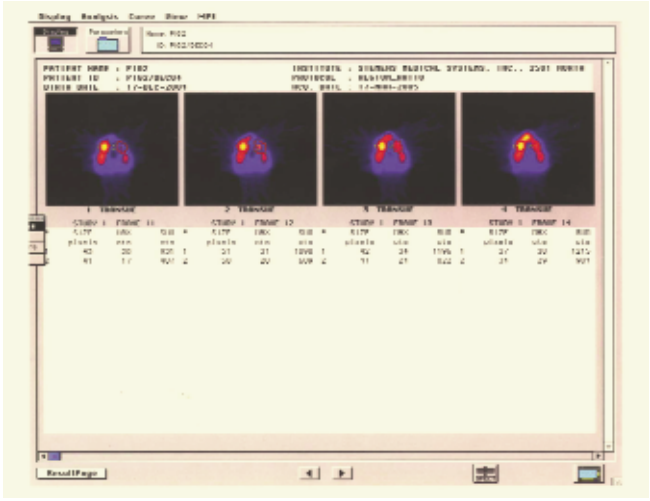

Fig. 1a: Osteoblastic activity at 8 weeks.

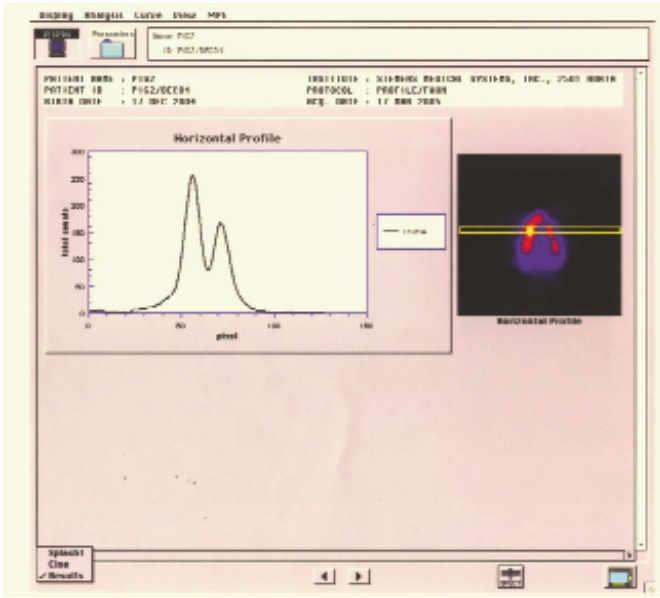

Fig. 1b: The graphical profile of osteoblastic activity of the sandwich side (SS) *versus* the interceed side (IS), together with the activity ratio. The IS has more activity than the SS at 8 weeks. Note that the actual left side of the pig is represented by the right side of the profile.

the 11th week (Fig. 7a–c) which retarded and obstructed bone formation into the 13th week, what we now term as osteobstruction.

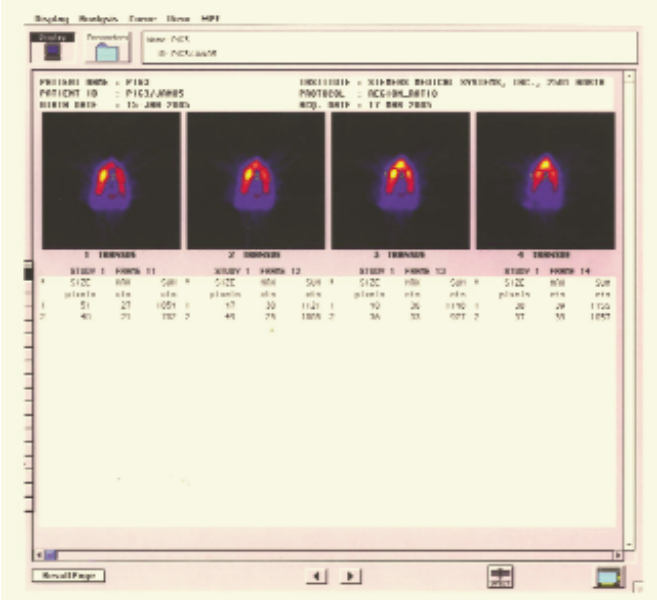

Fig. 2a: Osteoblastic activity at 11 weeks.

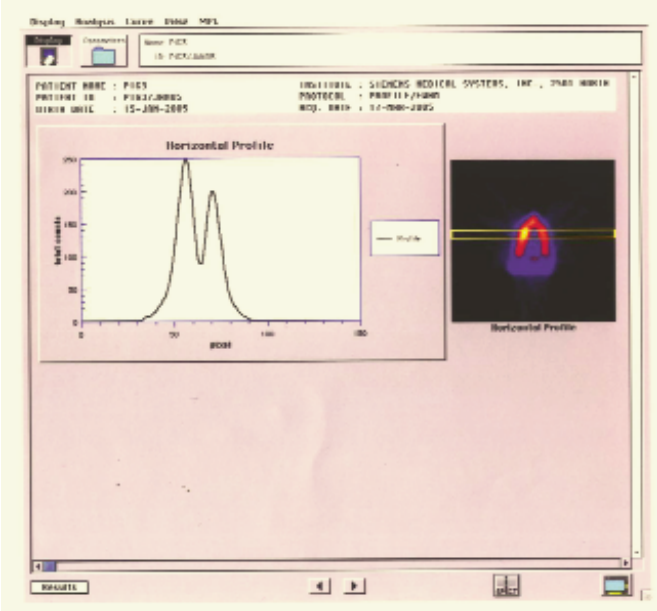

Fig. 2b: The graphical profile of osteoblastic activity of the sandwich side (SS) *versus* the interceed (IS) together with the activity ratio at 11 weeks. The interceed side still leads the SS at 11 weeks. Note that the actual left side of the pig's jaw is represented by the right side of the profile.

The governing mathematical equation for the osteobstruction in bone regeneration for the S-GTR model is the partial differential equation

$$\frac{\partial B}{\partial t} - \nabla \cdot (-D\nabla B) + \left(\frac{1-\gamma\varepsilon}{\gamma}\right) R\left(1 - \frac{B}{B_\infty}\right) B$$ [8] where B is the bone cell concentration; the first term on the right hand side of equation 8 represents bone cell motility (migration) and the second term is the bone cell proliferation at the graft site.

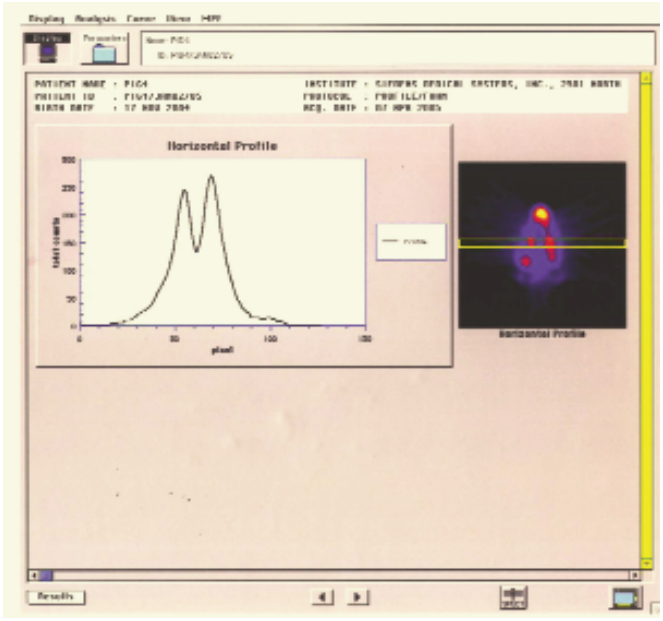

Fig. 3: The graphical profile of osteoblastic activity of the sandwich side (SS) *versus* the interceed side (IS) together with the activity ratio at 13 weeks. The osteoblastic activity in the sandwich side has now slightly overtaken the interceed side at 13 weeks. Note that the actual left side of the pig's jaw is represented by the right side of the profile.

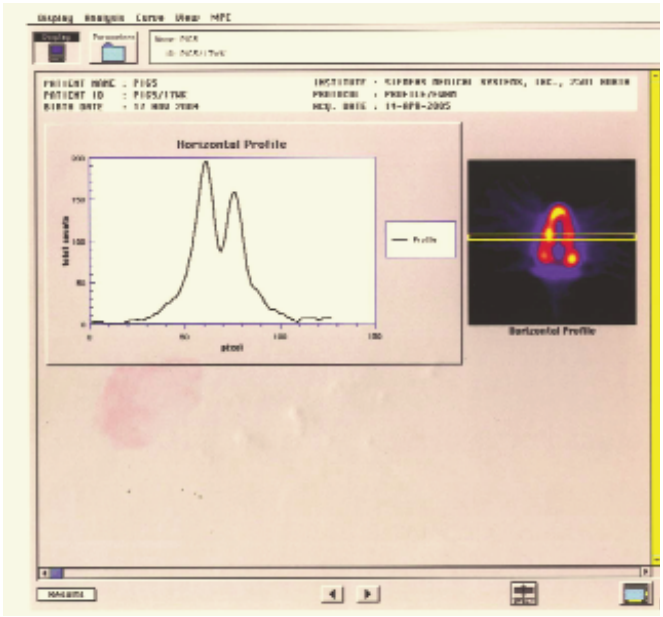

Fig. 4: The graphical profile of osteoblastic activity of the sandwich side (SS) *versus* the interceed side (IS) together with the activity ratio at 17 weeks. The IS still leads the SS in terms of osteoblastic activity at 17 weeks. Note that the actual left side of the pig's jaw is represented by the right side of the profile.

The partial differential equation governing the D-GTR model is $\frac{\partial B}{\partial t} = \nabla \cdot (D_2 \nabla B) + R_2\left(1 - \frac{B}{B_\infty}\right) B + \in \lambda_\infty$ where the last

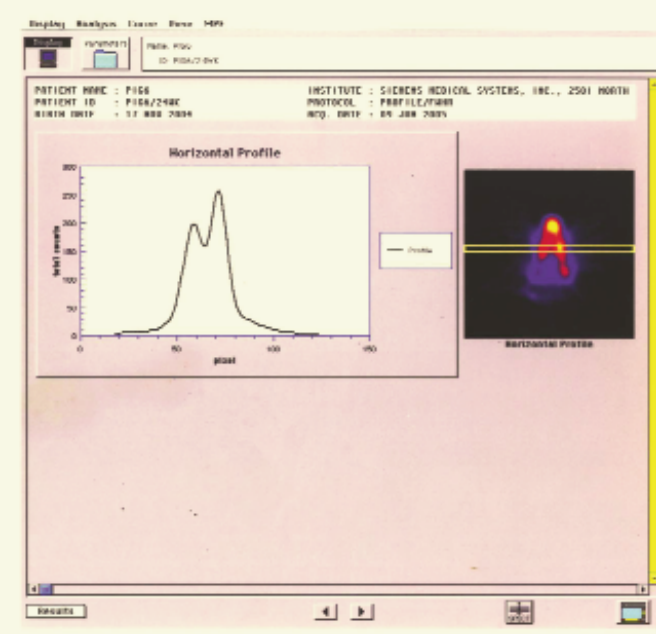

Fig. 5: The graphical profile of osteoblastic activity of the sandwich side (SS) *versus* the interceed side (IS), together with the activity ratio at 24 weeks. The sandwich side has finally exceeded the interceed side at 24 weeks.

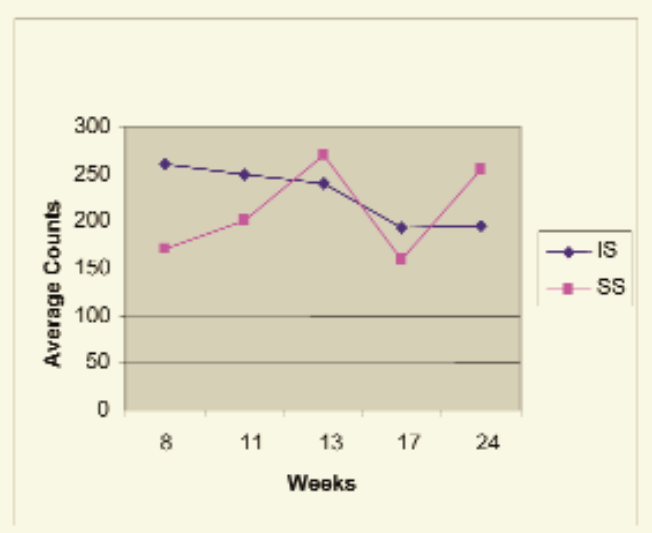

Fig. 6: The comparison of activity between the sandwich side (SS) and interceed side (IS). The average count of the IS with single guided tissue regeneration decreased from week 8 to week 24 although higher than the SS during weeks 8 and 11. The sandwich side linearly increased from weeks 8 to 13, but dropped in week 17 to overtake the IS at week 24, thus making the SS more superior in average count and osteoblastic activity overall when compared to the IS.

term on the right hand side of equation 9 represents the shock of resorption of membrane and some biochemical reactions.

Fig 7a: Medium power photomicrograph showing Bio-Oss in soft tissue representative of foreign body reaction (slide 22-06-49M; Stevenel's blue and van Gieson's picro fuchsin).

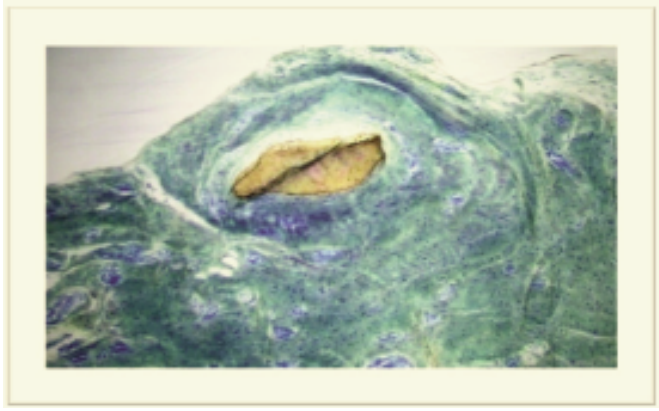

Fig 7b: High power photomicrograph showing Bio-Oss in soft tissue representative of foreign body reaction (slide 22-06-410H; Stevenel's blue and van Gieson's picro fuchsin).

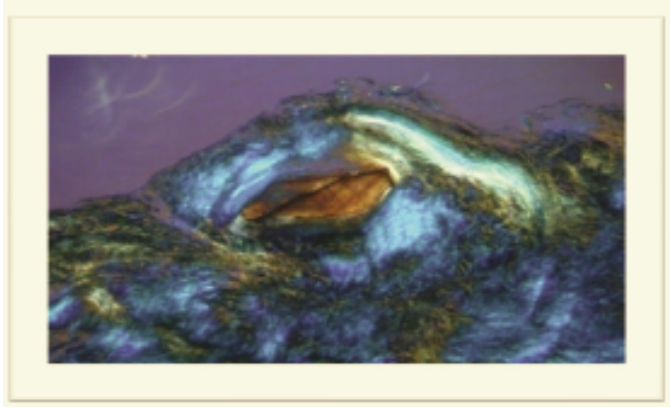

Fig 7c: Polarized view showing Bio-Oss in soft tissue representative of foreign body reaction (Slide 22-06-411H; Stevenel's blue and van Gieson's picro fuchsin).

Table: Comparative average count and activity ratio

	Pig No 2		Pig No 3		Pig No 4		Pig No 5		Pig No 6	
Mandibles	L	R	L	R	L	R	L	R	L	R
Time (weeks)	8 weeks		11 weeks		13 weeks		17 weeks		24 weeks	
Component of sandwich unit	IS	SS	IS	SS	IS	SS	IS	SS	IS	SS
Size of pixel										
Average count	260	170	250	200	240	270	194	160	195	255
Activity ratio	1:25		0:9		1:53		1:18		0:77	

SS = sandwich side; IS = interceed side

DISCUSSION

The significance of the GTR membrane is basically to confine the bone graft to the graft site. Obviously the thickness/type of membrane influences the osteoblastic activities and osseointegration of the graft material at the recipient site. Unfortunately, limitation exists because of limited observation in clinical, radiological, histological and histomorphometric evaluations, particularly because most experiments and observations are limited to twenty-four weeks and twenty-four months at most (or even less) despite the fact that osteoblastic potential may still remain at the site after this period. Osseointegration may be considered as a continuum since the graft material *eg* Bio-Oss may still remain within the regenerative site after two years.

Fortunately, in an extensive sequential animal experiment to validate the Ogunsalu sandwich regeneration technique using SPECT with correlative histological and histomorphometric evaluation, this experiment led to a coincidental finding of osteobstruction based on an interesting and unexpected observation of overtaking and re-overtaking phenomenon on SPECT during the sequential animal experiment evaluation. We strongly suspect that this is membrane type dependent and also the technique by which the membrane is utilized (S-GTR, D-GTR) as the bone graft used for the experiment was identical in both sites.

We note that the osteoblastic activities of the S-GTR site were more than that in the D-GTR site during the eighth–eleventh weeks. However, the D-GTR site suddenly slightly overtook the S-GTR site at the thirteenth week. This was the week that succeeded the foreign body reaction events on histology in the S-GTR site at the 11th week – a coincidental finding.

The histological event of foreign body reactions must have caused the retardation in osteoblastic activities in the D-GTR site. This sudden decreasing rate of bone formation in the D-GTR site from the 11th week into the 13th week and gradually fading out by the 17th week to allow the interceed (S-GTR) site to re-overtake the D-GTR site was a consequence of a histological event of foreign body reactions.

The above discussions are in agreement with the mathematical formulations. *Vis-a-vis* the 1st week to the 11th week, there were more osteoblastic activities at the S-GTR site than at the D-GTR site. Specifically in the 1st week of the experiment, the S-GTR site enabled a very high concentration of bone cell which allowed higher rate of osteoblastic activities, as the bone graft is not enclosed in a membrane sack; thus $R_1 > R_2 = R$ *ie* equation 4 implies $\frac{1+\xi\lambda_1}{1-\lambda_1} > 1$ [10] hence very high rates of bone cell proliferation is attained. In weeks later than the 11th week, there is the formation of soft tissue wall (foreign body reaction) at the S-GTR site which triggered reversal of bone cell migration from the S-GTR site; this is accounted for by the negative sign of diffusivity coefficient of bone cell motility in equation 8. This reversal of influx of bone cell to the S-GTR site led to retardation of osteoblastic activities at the site (osteobstruction). On the other hand, the diffusivity coefficient of bone cell motility in the case of the D-GTR site is always positive in equation 9, and we note that since bone graft is enclosed in the membrane sack, there is no rapid osteoblastic activity within the 1st week to the 11th week that could warrant accelerated osteoblastic activities at the D-GTR site. Hence, there is a slow and steady flux of bone cell into the D-GTR site which enabled slow and steady osteoblastic activities. Illustratively, S-GTR was 260 at the 8th week, 250 at the 11th week, and 240 at the 13th week, while the D-GTR gradually increased from 170 at the 8th week to 200 at the 11th week and 270 at the 13th week (Table; Figs. 1–6,).

Consequently, while there is osteoblastic activities retardation at the S-GTR site, there is a simultaneous acceleration of osteoblastic activities at the D-GTR site. Equation 9 also accommodates the sudden shock which produced a small decrease in osteoblastic activities at the D-GTR site (decrease from 270 at the 13th week to 160 at the 17th week). This shock is suspected to be the result of resorption of large quantities of membrane (approximately six times that of the S-GTR site) with some biochemical reactions in this site (Table; Figs. 1–6).

We strongly assert in this paper that the model equations could be utilized to predict, interpret and generalize the

osteobstruction phenomenon with desirable precisions, as solutions to the above equations are attainable.

CONCLUSIONS

Mathematical model has been utilized to explain the events that lead to osteobstruction (a newly identified bone regeneration mechanism) in the S-GTR side of the experimental animal in comparison with the D-GTR side. It is suggested that mathematical model be made mandatory in the explanation of bone regeneration mechanisms.

REFERENCES

1. Ogunsalu C, Ezeokoli C, Daisley H, Adogwa A, Watkins J, Archibald A et al. Single photon emission computerized tomography in the evaluation of the osteoblastic activities of a new bone regeneration technique: analysis of 12 mandibular sites in six experimental pigs. West Indian Med J 2008; **57:** 500–7.
2. Ogunsalu C, Rohrer M, Persad H, Archibald A, Watkins J, Daisley H et al. Single photon emission computerized tomography and histological evaluation in the validation of a new technique for the closure of oro-antral communication: an experimental study in pigs. West Indian Med J 2008; **57:** 166–72.
3. Ogunsalu C. Double-guided bone regeneration using the Ogunsalu sandwich regeneration technique: single photon emission computerized tomography, histology, and histomorphometric analysis. PhD thesis. St Augustine, Trinidad and Tobago: The University of the West Indies; 2009.
4. Murray JD. Mathematical biology; Vol I. 3rd ed. New York, NY: Springer; 2002.
5. Murray JD. Mathematical biology; Vol II. 3rd ed. New York, NY: Springer; 2003.
6. Prendergast PJ. Combining mechanoregulation algorithms for bone remodelling and tissue differentiation. In: Gonzalez Y, Cerrolaza M, eds. Bioengineering Modeling and Computer Simulation. Barcelona, Spain: CIMNE; 2007: 238–48.
7. Sengers BG, Please CP, Oreffo ROC. Experimental characterization and computational modeling of two-dimensional cell spreading for skeletal regeneration. JR Soc Interface 2007, **4:** 1107–17.
8. Shahaf G, Johnson K, Mehr R. B cell development in aging mice: lessons from mathematical modeling. International Immunology 2005, **18:** 31–9.
9. Takamizawa K, Niu S, Matsuda T. Mathematical simulation of unidirectional tissue formation in vitro transanastomotic endothelialization model. J Biomater Sc Polym Edin 1996, **8:** 323–34.
10. Savla U, Olson LE, Walters CM. Mathematical modeling of airway epithelial wound closure during cyclic mechanical strain. J Appl Physiol 2004, **96:** 566–74.
11. Maini PK, McElwain DL, Leavesley DI. Traveling waves in a wound healing assay. Appl Math Lett 2004; **17:** 575–80.
12. Vermolen FJ, van Baaren E, Adam JA. A simplified model for growth factor induced healing of circular wounds. Math Comp Modelling 2006; **44:** 887–98. [accessed December 2, 2009] Available from: http://ta.twi.tudelft.nl/TWA_Reports/05/05-04.pdf
13. Sherrat JA, Murray JD. Mathematical analysis of a basic model for epidermal wound healing. J Math Biology 1991, **29**: 389–404.
14. Murray JD. Mathematical biology II: spatial models and biomedical applications. New York: Springer-Varlag; 2004.
15. Filion J, Popel AS. A reaction-diffusion model of basic fibroblast growth factor interactions with cell surface receptors. Ann Biomed Eng 2004, **32:** 645–63.
16. Maggelakis SA. A mathematical model for tissue replacement during epidermal wound healing. Appl Math Modelling 2003, **27:** 189–96.
17. DiMilla PA, Barbee K, Lauffenburger DA. Mathematical model for the effects of adhesion and mechanics on cell migration speed. Biophys J 1991, **60:** 15–37.
18. Lauffenburger DA, Horwitz AF. Cell migration: a physically integrated molecular process. Cell 1996, **84**: 359–69.
19. Dee KC, Anderson TT, Bizios R. Osteoblast population migration characteristics on substrates modified with immobilized adhesive peptides. Biomaterials 1999, **20:** 221–7.
20. Erli HJ, Ruger M, Ragoss C, Jahnen-Dechant W, Hollander DA, Paar O et al. The effect of surface modification of a porous TiO2/perlite composite on the ingrowth of bone tissue in vivo. Biomaterials 2006, **27:** 1270–6.
21. Cukierman E, Pamkov R, Yamada KM. Cell interactions with three-dimensional matrices. Curr Opin Cell Biol 2002, **14:** 633–9.
22. Tranquillo RT, Zigmond SH, Lauffenburger DA. Measurement of the chemotaxis coefficient for human-neutrophils in the under-agarose migration assay. Cell Motil Cytoske 1988; **11:** 1–15.
23. O'Dea R. Multiphase modeling of tissue growth in dynamic culture conditions. PhD thesis. UK: University of Nottingham; 2007.
24. Maini PK, McElwain DL, Leavesley DI. Traveling wave model to interpret a wound-healing cell migration assay for human peritoneal mesothelial cells. Tissue Eng 2004, **10:** 475–82.
25. Sherrat JA, Marchant BP. Nonsharp traveling wave fronts in the Fisher equation with degenerate nonlinear diffusion. Appl Math Lett 1996; **9:** 33–9.